Genetic alterations of SENP6 in multiple myeloma disrupt genome and proteome stability, sensitizing to proteasome inhibition

Targeting the ubiquitin-proteasome system remains a mainstay in the treatment of multiple myeloma (MM), the second most common hematologic malignancy, driven by monoclonal plasma cell expansion. Despite major therapeutic advances over the past decades through proteasome inhibitors, immunomodulatory agents, monoclonal antibodies and, more recently, chimeric antigen receptor T-cell therapies and bispecific T-cell engagers, MM remains incurable and nearly all patients relapse. Molecular profiling has identified recurrent genetic alterations with varying clinical outcome, underscoring the disease's heterogeneity.[1] This genetic complexity emphasizes the need for personalized treatment strategies to overcome resistance and improve outcomes, particularly for patients with an adverse prognosis. Protein homeostasis in MM critically depends on the ubiquitin-proteasome system[2] and is further regulated by SUMOylation, a closely related post-translational protein modification, which orchestrates key cellular processes, such as cell cycle regulation, DNA repair, transcription and chromatin remodeling[3,4] by covalently attaching small ubiquitin-like modifiers (SUMO1, SUMO2, SUMO3) to target proteins. Like ubiquitylation, SUMOylation is controlled by a multi-step enzymatic cascade involving activating enzymes (SAE1/UBA2), conjugating enzymes (UBC9) and ligases, and is fully reversible through SUMO-specific proteases (SENP).[5] In cancer this balance is often disrupted and hyperactivation of the SUMO pathway is implicated in disease progression and associated with poor prognosis[6]

In this study we investigated the functional imbalance of dysregulated SUMOylation in MM by analyzing the large CoMMpass dataset for molecular alterations associated with SUMO pathway regulation. Deficiency of key SUMO proteases SENP6 and SENP7 emerged as a critical driver of aberrant SUMOylation dynamics, with recurrent loss of SENP6 being directly linked to adverse prognosis. SENP6 reconstitution markedly reduced cellular growth kinetics in SENP6-deficient MM, indicating a functional role for SENP6 as a tumor suppressor. Mechanistically, SENP6 loss resulted in the accumulation of DNA damage and misfolded proteins, thereby activating the unfolded protein response (UPR), increasing reliance on proteasomal degradation, and driving synthetic lethality to therapeutic proteasome inhibitors. We established that SENP6 is a functional biomarker and uncovered a mechanistic basis for enhanced efficacy of proteasome inhibitors in the prognostically unfavorable subgroup of SENP6-deficient MM patients. All experiments were performed in compliance with national guidelines and the principles of good scientific practice to ensure accuracy, reproducibility, and integrity of the data.

Aberrant activation of the SUMOylation pathway is a perceived hallmark of cancer.[6] Reflecting its role in tumor biology of MM, transcriptomic profiling of MM patients revealed an upregulation of the SUMOylation machinery compared to plasma cells from healthy donors (Figure 1A).[7] Analysis of the CoMMpass study, one of the largest and most comprehensive human MM datasets, showed a marked upregulation of the SUMO pathway in relapsed/refractory MM compared to newly diagnosed cases (Figure 1B).[1] Increased SUMOylation further correlated with advanced International Staging System stage (Figure 1C) and was linked to adverse clinical outcome (Figure 1D), collectively underscoring a prominent role for enhanced SUMOylation dynamics in MM biology and disease progression. As SENP activity is known to be a direct regulator of SUMOylation, we analyzed the interplay between the SUMO pathway and SUMO chain editing protease activity using a multivariable Cox model in the CoMMPass dataset. Notably, among SENP family members, only SENP6 and SENP7 can process poly-SUMO chains, and deficient poly-SUMO chain editing emerged as a key regulator driving adverse SUMOylation dynamics in MM (Figure 1E). Analysis of the CoMMpass dataset revealed recurrent arm level deletions of chromosome 6q, encompassing the *SENP6* locus, in ~15% of patients (Figure 1F), whereas *SENP7* was not affected by copy number loss (*Online Supplementary Figure S1A, B*). This was validated in an independent MM cohort, with 6q/*SENP6* deletions detected in 20% of cases (*Online Supplementary Figure S1C*)[8] and no evidence of 3q/*SENP7* loss (*Online Supplementary Figure S1D*). 6q/*SENP6* loss correlated with reduced *SENP6* mRNA expression (Figure 1G, *Online Supplementary Figure S1E*) and clinically, low *SENP6* levels were strongly associated with adverse prognosis in two independent datasets (Figure 1H, *Online Supplementary Figure S1F*).[9] Compared with myeloma precursor cells, *SENP6* expression was decreased at the time of disease onset (*Online Supplementary Figure S1G*).[10] It further declined with advanced International Staging System stage (Figure 1I) and was significantly lower in relapsed/refractory MM patients than in newly diagnosed MM cases (Figure 1J). Moreover, longitudinal analysis of paired bone marrow samples confirmed a progressive decline in *SENP6* expression from initial diagnosis to relapse (Figure 1K). Notably, the patients' treatment characteristics and high-risk genetic features were largely balanced across

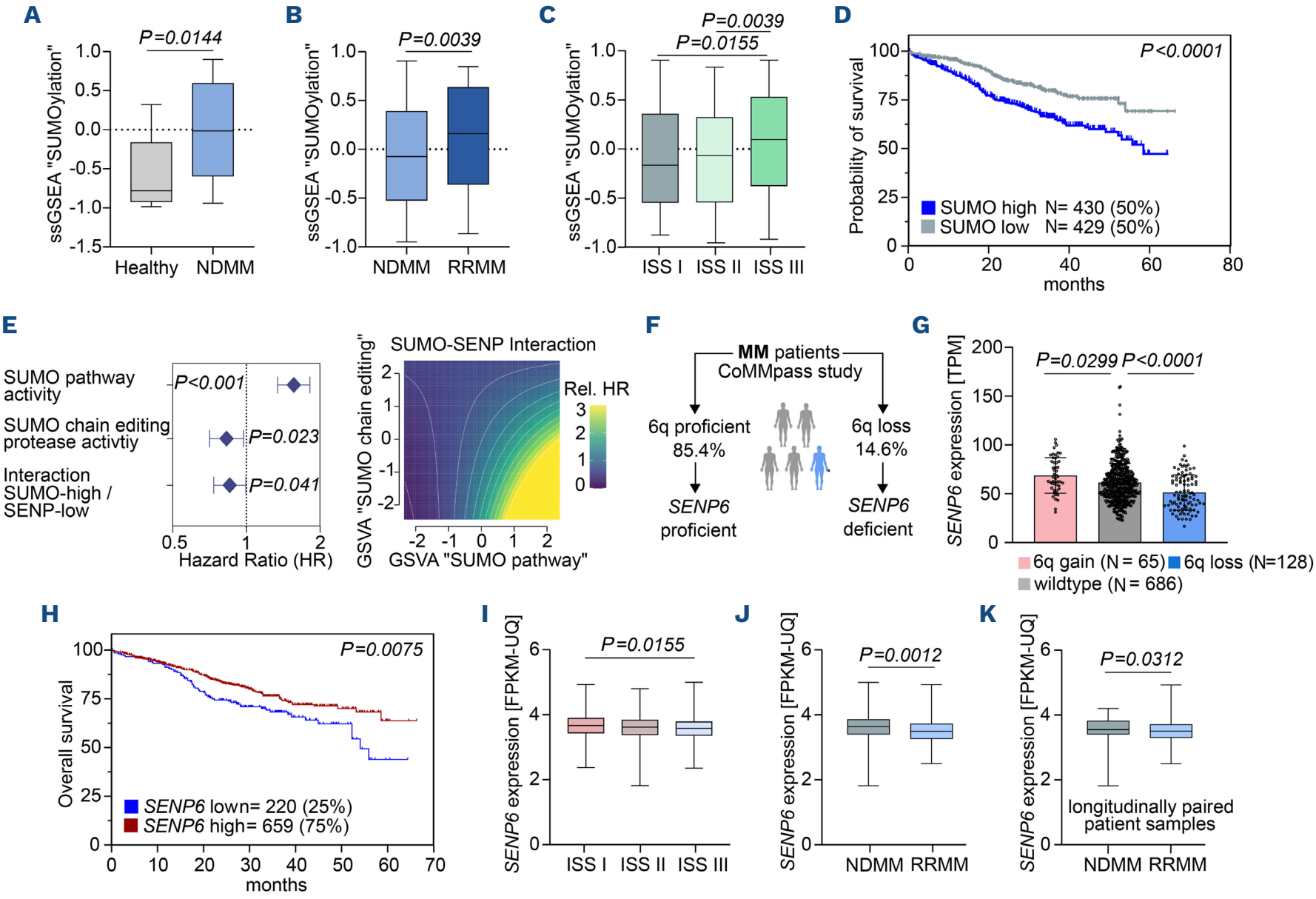

Figure 1. Enhanced SUMOylation dynamics driven by SENP6 loss are linked to disease progression and adverse prognosis in multiple myeloma. (A–C) Single-sample gene set enrichment analysis (ssGSEA) enrichment scores for the Reactome gene set "SUMOylation" in healthy donors (N=6) *versus* patients with newly diagnosed multiple myeloma (NDMM, N=170) (Chauhan *et al.*) (A), NDMM (N=764) *versus* relapsed/refractory multiple myeloma (RRMM, N=80) (B) and across International Staging System (ISS) stages I–III (C) in the CoMMpass cohort. (D) Kaplan–Meier overall survival curve of multiple myeloma (MM) patients in the CoMMpass cohort stratified by ssGSEA enrichment scores for the Reactome gene set "SUMOylation". (E) Forest plot of interaction Cox analysis displaying hazard ratios of depicted z-standardized reactome pathways in the CoMMpass cohort. Pathway interaction surface visualizing the joint effect of high SUMO pathway and low SUMO chain editing protease activity on overall survival. (F, G) *SENP6* copy number alterations (F) and corresponding expression (G) in the CoMMpass cohort. Wildtype (N=686); 6q del (N=128); 6q gain (N=65). (H) Kaplan–Meier overall survival curve of MM patients in the CoMMpass cohort stratified by SENP6 expression. (I–K) *SENP6* expression of MM patients in the CoMMpass cohort across ISS stage (I), in NDMM *versus* RRMM (J), and in paired patients' samples at diagnosis and relapse (N=47) (K). Box and whisker plots indicate minimum to maximum distribution and the mean. *P* values calculated by a Mann–Whitney U tests (A, B, J), Kruskal–Wallis analysis of variance with the Tukey *post-hoc* test (C, I), Wilcoxon matched-pairs test (K), or log-rank test (D, H). GSVA: gene set variation analysis; TPM: transcripts per million; FPKM-UQ: fragments per kilobase of transcript per million mapped reads upper quartile.

subgroups of patients with different *SENP6* expression (*Online Supplementary Figure S1H, I*). Collectively, these data demonstrate that enhanced SUMOylation in MM is linked to recurrent *SENP6* loss, which is associated with disease progression and a poor clinical outcome.

To establish mechanistic models, we analyzed the Cancer Cell Line Encyclopedia (CCLE) and identified 11 MM cell lines with genetic *SENP6* loss and 17 with an intact *SENP6* locus (Figure 2A). Ectopic reconstitution of SENP6 in SENP6-deficient AMO-1 and L-363 cells significantly impaired cellular growth (Figure 2B, C), indicating a functional role for SENP6 as a tumor suppressor in MM. Given the inverse correlation between SENP6 expression and SUMOylation in MM patients, we next assessed the functional impact of SENP6 expression on cellular SUMO homeostasis. SENP6 reconstitution in AMO-1 cells markedly reduced SUMO2/3 and SUMO1 conjugates (Figure 2D), whereas CRISPR/Cas9-mediated *SENP6* depletion (*SENP6*^{KD}) in three cell lines with intact *SENP6* loci (MM.1S, NCI-H929, OPM-2) resulted in notable accumulation of SUMO2/3- and SUMO1-conjugated proteins (*Online Supplementary Figure S2A, S2B*). This effect was more pronounced for SUMO2/3 conjugates than for SUMO1, consistent with the preferential affinity of SENP6 for SUMO2/3 conjugates. Furthermore, SENP6 loss resulted

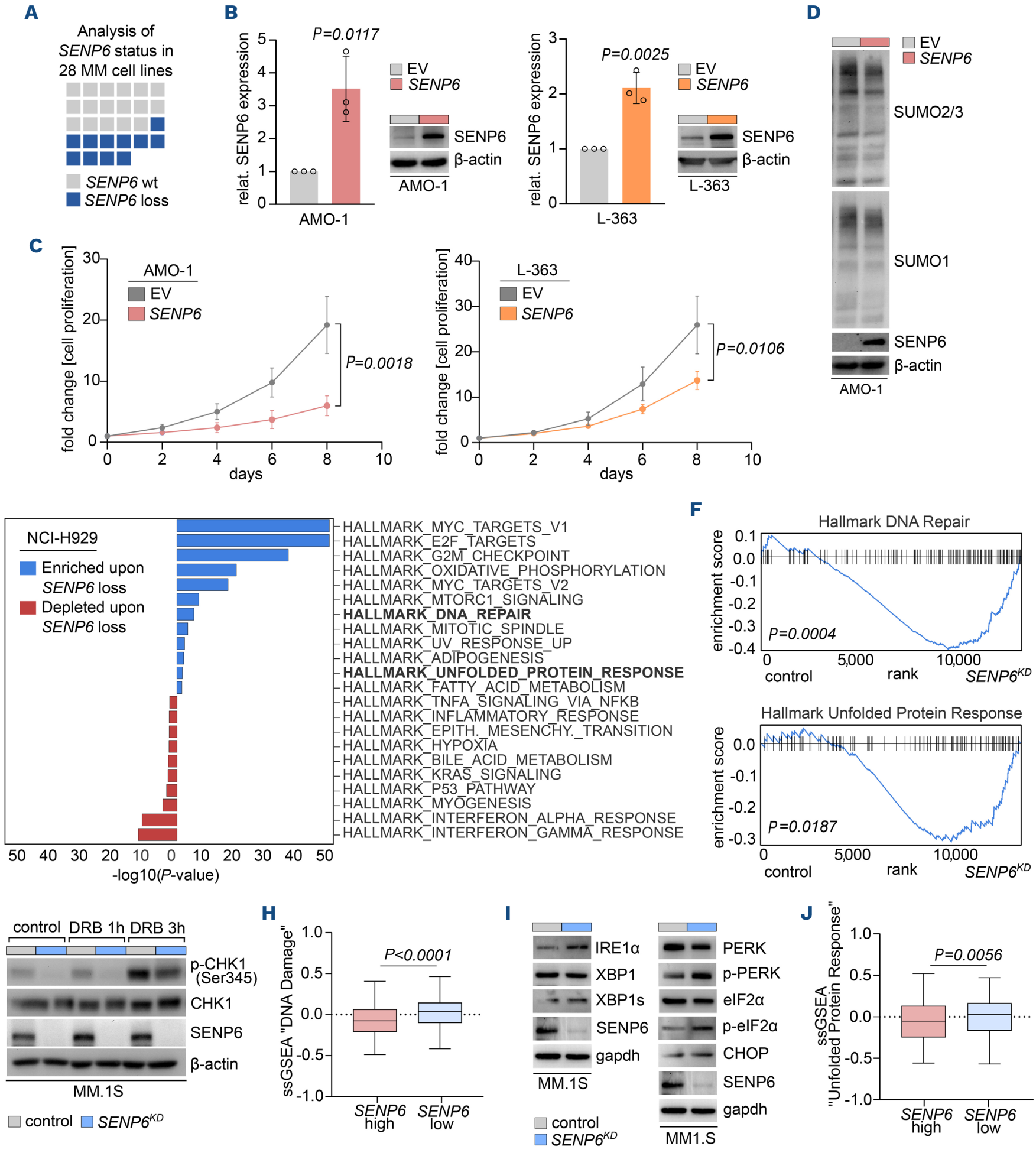

Figure 2. SENP6 safeguards SUMO homeostasis and protects genome stability and proteome integrity in multiple myeloma. (A) Expression analysis of *SENP6* mRNA in multiple myeloma (MM) cell lines (N=28). (B) Immunoblot analysis of SENP6 protein expression upon *SENP6* reconstitution *versus* empty vector (EV) transduction in AMO-1 and L-363 cells. SENP6 protein expression was normalized to β-actin for quantification. (C) Analysis of cell proliferation upon *SENP6* reconstitution *versus* EV transduction in AMO-1 and L-363 cells. (D) Immunoblot analysis of global SUMO2/3 and SUMO1 modification in AMO-1 cells upon *SENP6* reconstitution *versus* EV transduction. (E, F) Gene set enrichment analysis (GSEA) of NCI-H929 control *versus* *SENP6*^{KD} (E), highlighting enrichment of DNA damage response (DDR) and unfolded protein response (UPR)-related pathways (F). (G) Immunoblot analysis of DDR-related proteins in MM.1S control and *SENP6*^{KD} following doxorubicin (0.5 μM) treatment at the indicated time-

Continued on following page.

points. (H) Single-sample GSEA enrichment scores for the hallmark "DNA damage" gene set in *SENP6*^{low} (N=211) *versus* *SENP6*^{high} (N=633) samples from the CoMMpass cohort. (I) Immunoblot analysis of UPR markers in MM.1S control and *SENP6*^{KD} cells. (J) Single-sample GSEA enrichment scores for the hallmark "UPR" gene set in *SENP6*^{low} (N=211) *versus* *SENP6*^{high} (N=633) samples from the CoMMpass cohort. Data represent the mean ± standard deviation in (B) and (C). Box and whisker plots indicate minimum to maximum distribution and the mean in (H) and (J). *P* values were calculated by unpaired *t* tests (B, C), the Kolmogorov–Smirnov test (F) and Mann–Whitney U tests (H, J). wt: wild-type; relat.: relative; DRB: daunorubicin.

in accumulation of high molecular weight SUMO2/3 conjugates, indicative of impaired poly-SUMO chain editing.[5] Consistently, gene set enrichment analysis (GSEA) of patients' samples revealed a significant enrichment of the SUMO conjugation pathway in SENP6-deficient MM (*Online Supplementary Figure S2C*). Together, these data identify SENP6 as a tumor suppressor and key regulator of SUMO homeostasis in MM.

To systematically investigate the molecular consequences of SENP6 loss in MM, we performed transcriptome profiling of SENP6-depleted MM cells. GSEA revealed enrichment of oncogenic signatures, including "DNA repair" and "unfolded protein response", indicating increased DNA damage and endoplasmic reticulum (ER) stress upon SENP6 deficiency (Figure 2E, 2F, *Online Supplementary Figure S2D, E*). In line with the role of SENP6 in chromatin organization and the DNA damage response (DDR),[11-13] SENP6 depletion impaired DDR signaling, as shown by reduced CHK1 phosphorylation upon DNA-damaging doxorubicin treatment (Figure 2G). Moreover, a marked increase in γH2AX phosphorylation was detected, indicating a pronounced accumulation of DNA double-strand breaks (*Online Supplementary Figure S2F*). Consistently, analysis of the CoMMpass dataset reinforced this link, revealing a "DNA damage" signature in SENP6-deficient MM patients (Figure 2H). Moreover, SENP6-deficient MM cell lines displayed significantly more co-occurring copy number alterations than SENP6-proficient cell lines (*Online Supplementary Figure S2G, H*), further supporting its role as a critical guardian of genome stability in MM. Plasma cells depend on an efficient proteostasis network in the ER to sustain immunoglobulin synthesis, folding, and secretion, rendering them particularly sensitive to ER stress.[14] Defective DDR and increased genomic instability promote accumulation of misfolded and unfolded proteins in the ER,[15] thereby triggering the UPR as a compensatory response to restore protein homeostasis.[16] In line with increased genotoxic stress, SENP6-deficient MM cells showed robust UPR activation compared to controls (Figure 2E, F, *Online Supplementary Figure S2E*). Immunoblot analysis confirmed elevated UPR signaling, including increased IRE1α expression, enhanced XBP1 splicing, and PERK phosphorylation (Figure 2I, *Online Supplementary Figure S2I*). To assess the clinical relevance, single-sample GSEA of the CoMMpass dataset revealed enrichment of the UPR signature in SENP6-deficient MM patients (Figure 2J). We here identify SENP6 as a central regulator of ER homeostasis and stress adaptation in MM, highlighting its critical role in maintaining proteostasis through modulation of the UPR. Together, our data position SENP6 as a dual guardian of genome integrity and protein homeostasis in MM by coordinating DDR signaling and ER integrity.

To comprehensively explore therapeutic vulnerabilities to standard-of-care treatments in the clinically unfavorable subgroup of SENP6-deficient MM, we performed a high-throughput image-based drug screen (pharmacoscopy) using the Operetta® CLS microplate imager platform (Figure 3A). Pharmacoscopy enables highly precise quantification of diverse cellular parameters and markers with unprecedented accuracy due to the large number of events monitored.[17] In detail, control and SENP6-deficient cells were exposed to increasing concentrations of standard MM drugs for 72 hours, followed by automated imaging and analysis. Leveraging the open-access drug screening analysis pipeline Breeze2.0,[18] SENP6-deficient cells showed a marked increase in sensitivity to proteasome inhibitors (bortezomib, carfilzomib) (Figure 3B, C). Mechanistically, SENP6 loss impairs DDR and activates the UPR. Misfolded proteins are primarily cleared via ER-associated degradation, which involves retrograde translocation to the cytosol followed by 26S proteasome-mediated degradation.[19] Consequently, SENP6-deficient MM cells became increasingly dependent on proteasomal function to maintain ER integrity, making them particularly vulnerable to proteasome inhibitors. Furthermore, SENP6-depleted MM cells displayed enhanced sensitivity to cyclophosphamide and etoposide, both of which induce DNA damage and disproportionately impact cells with impaired cell-cycle checkpoint activation as observed for SENP6 deficiency. In contrast, SENP6-deficient MM cells showed only marginal responses to dexamethasone and no change in response to melphalan or immunomodulatory agents (Figure 3B, C). These findings were validated across an informative MM cell line panel. Accordingly, SENP6 depletion increased sensitivity to both bortezomib and carfilzomib treatment (Figure 3D-G, *Online Supplementary Figure S3A, B*), consistent with enhanced apoptosis rates (*Online Supplementary Figure S3C, D*). In support of our findings, ectopic SENP6 reconstitution in AMO-1 and L-363 cells conferred resistance to treatment with proteasome inhibitors (*Online Supplementary Figure S3E-H*). In summary, these data provide a mechanistic rationale for enhanced efficacy of proteasome inhibition in the subgroup of patients with SENP6-depleted MM.

In conclusion, in this study, we uncovered a critical role for enhanced SUMOylation dynamics in MM biology. By integrating patients' data with mechanistic studies, we identified recurrent deletions of *SENP6* as a molecular feature of a clinically unfavorable MM subgroup. Functionally, loss of

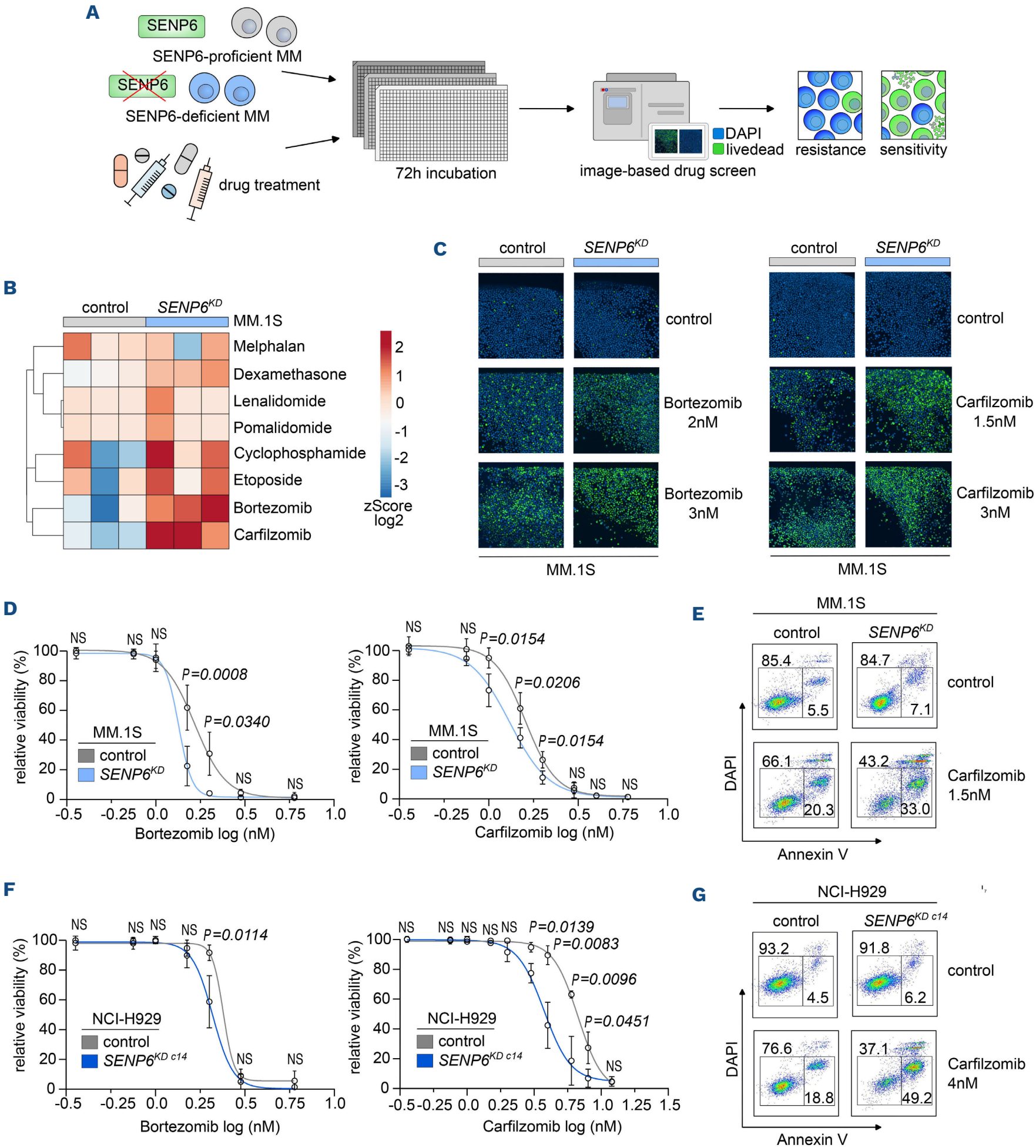

Figure 3. High-throughput image-based drug screening discovers synthetic lethality to proteasome inhibition in SENP6-deficient multiple myeloma. (A) Workflow of the high-content image-based drug testing platform (Operetta) to exploit treatment strategies in SENP6-deficient multiple myeloma (MM). Cells were stained with DAPI and live/dead stain before imaging. (B) Drug sensitivity scores of MM.1S control and *SENP6*^{KD} cells upon treatment with the indicated drugs and as outlined in (A) were calculated by the BREEZE drug screen analysis pipeline. The heatmap was generated by the ClustVis data visualizing tool. (C) Representative images of MM.1S control and *SENP6*^{KD} cells upon treatment with the indicated concentrations of bortezomib and carfilzomib for 72 hours. (D, F) Dose–response curves for bortezomib and carfilzomib in control and *SENP6*^{KD} MM.1S (D) and NCI-H929 (F) cells. Cells were treated for 72 hours and viability was assessed by DAPI-based flow cytometry. (E, G) Representative DAPI-annexin-V dot plots for control and carfilzomib shown in (E, G). Dose–response curves represent mean ± standard deviation (D, F). *P* values were determined by an unpaired *t* test (D, F). DAPI: 4',6-diamidino-2-phenylindole.

SENP6 drives excessive poly-SUMOylation, impairing DNA repair, genomic stability, and protein homeostasis. These vulnerabilities activate the UPR and increase reliance on proteasomal degradation, creating synthetic lethality to therapeutic proteasome inhibitors. Despite this initial proteasome inhibitor vulnerability, SENP6-deficient MM patients exhibit poorer outcomes, indicating that additional mechanisms may limit therapeutic efficacy over time. Mechanistically, we demonstrate a critical role for SENP6 in preserving genomic integrity by guarding DNA repair. Maintenance of genomic stability is essential for cellular homeostasis, and its loss fosters oncogenic evolution. Accordingly, SENP6 deficiency is associated with increased genomic instability in MM, potentially driving tumor evolution and progression.

Authors

Frederik Herzberg,[1,2*] Michael Korenkov,[1,2*] Konstandina Isaakidis,[1,2] Chuanbing Zang,[1,2] Matthias Wirth,[1-4] Stefan Müller,[4,5] Ulrich Keller[1,2,4,6,7] and Uta M. Demel[1,2,8]

[1]Department of Hematology, Oncology and Cancer Immunology, Campus Benjamin Franklin, Charité - Universitätsmedizin Berlin, corporate member of Freie Universität Berlin and Humboldt-Universität zu Berlin, Berlin; [2]Max-Delbrück-Center for Molecular Medicine, Berlin; [3]Department of General, Visceral and Pediatric Surgery, University Medical Center Göttingen, Göttingen; [4]German Consortium for Translational Cancer Research (DKTK), partner site Berlin, German Cancer Research Center (DKFZ), Heidelberg; [5]Institute of Biochemistry II, Goethe University Frankfurt, Medical School, Frankfurt; [6]National Center for Tumor Diseases (NCT), partner site Berlin, German Cancer Research Center (DKFZ), Heidelberg; [7]Cluster of Excellence ImmunoPreCept, Charité - Universitätsmedizin Berlin, Berlin and [8]Clinician Scientist Program, Berlin Institute of Health (BIH), Berlin, Germany

**FH and MK contributed equally as first authors.*

Correspondence:
U.M. DEMEL - uta.demel@charite.de

https://doi.org/10.3324/haematol.2025.288863

Received: September 4, 2025.
Accepted: November 24, 2025.
Early view: December 4, 2025.

Disclosures

No conflicts of interest to disclose.

Contributions

FH, MK, UK and UMD conceived and designed the study. FH, MK, KI, CZ, MW, SM, UK and UMD acquired and/or analyzed and interpreted data. FH, MK, UK and UMD drafted the manuscript. All authors revised the manuscript for important intellectual content and approved the final version submitted for publication.

Acknowledgments

We gratefully acknowledge Marlon Schielin for his excellent technical assistance and support with all experiments.

Funding

This work was supported by Wilhelm Sander Stiftung grant 2024.109.1 to UMD and 2017.048.2 to UK; Deutsche Forschungsgemeinschaft (DFG) grant KE222/11-1 project number 508460329 to UK, KE222/10-1 project number 494535244 to UK and SM, and WI 6148/1-1 project number 529255113 to MW; Deutsche Krebshilfe grants 70111944, 70114724 and 70116097 to UK, 70114724 to UK and SM, and 70115444 to MW; Else Kröner-Fresenius-Stiftung grant 2024_KEA.07 to UMD; Hector Stiftung grant M2506 to UK, M2408 to MW, and Stiftung Charité to UK. UMD is a participant in the BIH-Charité Clinician Scientist program funded by the Charité-Universitätsmedizin Berlin und BIH.

Data-sharing statement

The RNA-sequencing data generated in this study have been stored on the GEO server with project accession number GSE303255. Further data reported in this paper will be shared by the lead contact upon request.

References

1. Skerget S, Penaherrera D, Chari A, et al. Comprehensive molecular profiling of multiple myeloma identifies refined copy number and expression subtypes. Nat Genet. 2024;56(9):1878-1889.
2. Lub S, Maes K, Menu E, De Bruyne E, Vanderkerken K, Van Valckenborgh E. Novel strategies to target the ubiquitin proteasome system in multiple myeloma. Oncotarget. 2016;7(6):6521-6537.
3. Flotho A, Melchior F. Sumoylation: a regulatory protein modification in health and disease. Annu Rev Biochem. 2013;82:357-385.
4. Vertegaal ACO. Signalling mechanisms and cellular functions of SUMO. Nat Rev Mol Cell Biol. 2022;23(11):715-731.
5. Kunz K, Piller T, Muller S. SUMO-specific proteases and isopeptidases of the SENP family at a glance. J Cell Sci. 2018;131(6):jcs211904.
6. Seeler JS, Dejean A. SUMO and the robustness of cancer. Nat Rev Cancer. 2017;17(3):184-197.
7. Chauhan D, Tian Z, Nicholson B, et al. A small molecule inhibitor of ubiquitin-specific protease-7 induces apoptosis in multiple myeloma cells and overcomes bortezomib resistance. Cancer Cell. 2012;22(3):345-358.

8. Chapman MA, Lawrence MS, Keats JJ, et al. Initial genome sequencing and analysis of multiple myeloma. Nature. 2011;471(7339):467-472.
9. Hanamura I, Stewart JP, Huang Y, et al. Frequent gain of chromosome band 1q21 in plasma-cell dyscrasias detected by fluorescence in situ hybridization: incidence increases from MGUS to relapsed myeloma and is related to prognosis and disease progression following tandem stem-cell transplantation. Blood. 2006;108(5):1724-1732.
10. Boiarsky R, Haradhvala NJ, Alberge JB, et al. Single cell characterization of myeloma and its precursor conditions reveals transcriptional signatures of early tumorigenesis. Nat Commun. 2022;13(1):7040.
11. Wagner K, Kunz K, Piller T, et al. The SUMO isopeptidase SENP6 Functions as a rheostat of chromatin residency in genome maintenance and chromosome dynamics. Cell Rep. 2019;29(2):480-494.e485.
12. Schick M, Zhang L, Maurer S, et al. Genetic alterations of the SUMO isopeptidase SENP6 drive lymphomagenesis and genetic instability in diffuse large B-cell lymphoma. Nat Commun. 2022;13(1):281.
13. Liebelt F, Jansen NS, Kumar S, et al. The poly-SUMO2/3 protease SENP6 enables assembly of the constitutive centromere-associated network by group deSUMOylation. Nat Commun. 2019;10(1):3987.
14. Vincenz L, Jager R, O'Dwyer M, Samali A. Endoplasmic reticulum stress and the unfolded protein response: targeting the Achilles heel of multiple myeloma. Mol Cancer Ther. 2013;12(6):831-843.
15. Gonzalez-Quiroz M, Blondel A, Sagredo A, Hetz C, Chevet E, Pedeux R. When endoplasmic reticulum proteostasis meets the DNA damage response. Trends Cell Biol. 2020;30(11):881-891.
16. Hetz C, Zhang K, Kaufman RJ. Mechanisms, regulation and functions of the unfolded protein response. Nat Rev Mol Cell Biol. 2020;21(8):421-438.
17. Kropivsek K, Kachel P, Goetze S, et al. Ex vivo drug response heterogeneity reveals personalized therapeutic strategies for patients with multiple myeloma. Nat Cancer. 2023;4(5):734-753.
18. Potdar S, Ianevski F, Ianevski A, et al. Breeze 2.0: an interactive web-tool for visual analysis and comparison of drug response data. Nucleic Acids Res. 2023;51(W1):W57-W61.
19. Obeng EA, Carlson LM, Gutman DM, Harrington WJ Jr, Lee KP, Boise LH. Proteasome inhibitors induce a terminal unfolded protein response in multiple myeloma cells. Blood. 2006;107(12):4907-4916.